



Published in final edited form as:

J Int Soc Respir Prot. 2017 December 31; 34(2): 81–94.

Work of Breathing for Respiratory Protective Devices: Method Implementation, Intra-, Inter-Laboratory Variability and Repeatability

William P. King¹, Margaret Sietsema², Caitlin McClain¹, Susan Xu¹, Helion Dhrimaj³

¹National Institute for Occupational Safety and Health, National Personal Protective Technology Laboratory, Pittsburgh, Pennsylvania 15236

²University of Illinois at Chicago, Chicago IL

³North Carolina State University, Raleigh, NC

Abstract

As part of development of performance standards, the International Organization for Standardization (ISO) technical committee, ISO/TC 94/SC 15 Respiratory protective devices (RPD), adopted work of breathing (WOB) to evaluate airflow resistance for all designs (classes) of respiratory protective devices. The interests of the National Institute for Occupational Safety and Health's (NIOSH) National Personal Protective Technology Laboratory (NPPTL) are to compare the proposed WOB method and results for current RPD with those for present resistance methods. The objectives here were to assemble a method to meet the ISO SC15 standards, validate operation and conformance, and assess repeatability of WOB measurements for RPD. WOB method implementation and use followed standards ISO 16900–5:2016 and ISO 16900–12:2016. Volume-averaged total work of breathing (WOB_T/V_T where V_T is tidal volume) determined for standard orifices was analyzed for variation and bias. After fabrication and assembly, the method gave preliminary verification orifice results that met ISO requirements and were equivalent to those from other laboratories. Evaluation of additional results from RPD testing showed tidal volume and frequency determined compliance. Appropriate adjustments reduced average absolute bias to 1.7%. Average coefficient of variation for WOB_T/V_T was 2.3%. Over 97% of results obtained during significant use over time met specifications. WOB_T/V_T for as-received air-purifying and supplied-air RPD were repeatable ($p < 0.05$). WOB_T/V_T for unsealed half mask air-purifying RPD was an average of 31% lower compared to sealed. When experimental parameters were appropriately adjusted, the ISO WOB method implemented by NIOSH NPPTL consistently provided ISO-compliant verification WOB_T/V_T . Results for appropriately sealed RPD were reproducible.

*Corresponding author bwq5@cdc.gov.

Disclaimer

The findings and conclusions of this article are those of the authors and do not necessarily represent the views of the National Institute for Occupational Health and Safety. Mention of a commercial product or trade name does not constitute endorsement by the National Institute for Occupational Safety and Health.

Keywords

work of breathing; resistance; respirator; respiratory protective device

INTRODUCTION

In an initial study of the effect of respiratory protective devices (RPD) on wearers, work of breathing (WOB) was proposed for assessment of airflow resistance (Silverman 1943). Although WOB was (and continues to be) used in the study of physiologic effects of RPD, it was not widely adopted in RPD standards. Even though volume-averaged WOB, which is essentially average pressure from pressure-volume (P-V) data (see below), reflects conditions over the entire breathing volume, the simplicity of a single airflow resistance measurement at constant flow for air-purifying RPD likely outweighed the added effort to apply physiologic waveforms, acquire pressure-volume data, and calculations to obtain WOB.

The impact of RPD airflow resistance on wearer performance at high work rates has been documented (Bentley 1973), (Caretto 2006). Dynamic and non-linear flow effects contribute to airflow resistance, which for the latter is significant at high work rates. Such contributions are readily seen in WOB (Shykoff and Warkander 2011) where constant flow resistance measurements are limited. Since the 1970s, methods and limits for WOB and related parameters have been developed and used for underwater breathing apparatus (*e.g.* CEN 2003). With improved technology (*e.g.* programmable servomotors in place of cams, high-speed digital electronic data acquisition replacing strip chart recorders, and software for planimeters), the effort to obtain P-V data and derive WOB and related parameters is now comparable to constant flow measurement. Owing to these factors (wider applicability, established methods, and feasibility), the ISO technical committee, ISO/TC 94/SC 15 Respiratory Protective Devices, proposed physiologically-based limits for volume-averaged WOB and related parameters for all RPD design classes (ISO 2012) using standard methodology (ISO 2016A).

The method prescribes a breathing machine (ISO 2016B) [or metabolic simulator for closed-circuit designs (ISO 2015A)] to provide a sinusoidal breathing waveform via a trachea tube assembly inside a headform (Figure 1) to affixed RPD, as pressure at the trachea inlet, P , and breathing volume, V , are recorded. From the P-V loop (so-named for the figure produced when plotted *e.g.* Figure 2 middle graph), WOB is obtained by integrating P over V , $\int P \Delta V$, and volume-averaged WOB by dividing by breathing volume (WOB/ V). Relationships for WOB and related P-V parameters: maximum expiratory pressure, minimum inspiratory pressure, and elastance (ISO 2012) are given in Appendix A.

Our aim at the NIOSH NPPTL was to compare WOB and current resistance evaluation methods. This required implementing a WOB test method to meeting ISO requirements and was carried out in steps: 1) Assemble the method to achieve preliminary results in agreement with expected values, variability (standard deviation) and bias. 2) Validate acceptability for significant number of results from method use and, as necessary, evaluate the need for adjustments. 3) Evaluate repeatability of RPD results. As suggested in the ISO headform

task group, implementation issues are included as guidance for developing WOB evaluation of RPD in Appendix B. WOB and related parameters determined for RPD and method comparisons will be the subject of later reports.

MATERIALS AND METHODS

The work of breathing method configuration followed ISO standard 16900–5:2016 (ISO 2016A).

Breathing Machine

NIOSH / NPPTL used a Warwick Technology dynamic digital breathing machine (Figure 1B). The device uses a brushless servo motor/electric cylinder to drive an aluminum piston enclosed in a steel cylinder. (Warwick Technology 2013) A linear potentiometer is used for position feedback to the electric cylinder controller. Software written in LabVIEW™ (National Instruments, Austin, TX) provides several functions. Two functions were used primarily: Create simple waveform generates for inputs of tidal (displacement) volume and frequency, a waveform file (a series of waveform volumes) to produce sinusoidal breathing machine output. Waveform with DAQ operates the breathing machine using a selected waveform file, and collects voltage data from the breathing machine and peripheral sources at a selected rate and duration. The waveform file volume, potentiometer voltage, pressure transducer output voltage and (when added later) laser position sensor voltage output were recorded at 100 points per second for 60 seconds. The pressure-decay leak check (ISO 16900–5:2016 Section 4.3) was used to assess leak tightness (ISO 2016A).

Headforms and Trachea Tube Assembly

The ISO RPD headforms, specified in ISO/TS 16976–2:2015 (ISO 2015B), were 3-D printed in acrylonitrile butadiene styrene (ABS) thermoplastic using files from ISO 16900–5:2016 (ISO 2016A). To achieve reasonable build times, a coarse nozzle, 0.40 mm (0.016 inch) diameter, was used. Due to the porous nature of 3D-printed solids, a polyurethane sealant (Minwax™ fast-drying polyurethane) was applied externally to the lightly sanded headforms to both prevent air leakage through the headform and reduce the surface roughness. Headform verification dimensions used to identify head forms (Table I in ISO 16900–5:2016), were unchanged after sanding and sealing. The trachea tube assembly (Figure 1B) and breathing machine (with a pipe nipple with flange sealed over the inlet) were connected with a short length of heavy-walled Tygon® tubing. An internal trachea support and neck extension/headform support were added to accommodate the connection (Figure 1A).

Piston Position

A non-contact laser-triangulation position sensor (Acuity AR700, Schmitt Measurement Systems, Portland OR) was used to provide piston position information. [A linear voltage displacement transducer (LVDT) has also been used for direct piston position (Warkander 2015). The LVDT manufacturer has replaced these devices with linear inductive position sensors (Positek 2017).]

Pressure Measurements

A pressure transducer (DP-45–24) and controller (CD23) (Validyne Engineering Northridge, CA) provided pressure measurements. These were calibrated against a Datum 2000 manometer (Setra Systems, Foxboro, MA) calibrated against the U. S. National Institute of Standards and Technology - traceable standards. The transducer was connected via 3mm (1/8 inch) ID silicone tubing to the pitot ring, an annular arrangement of 14 1mm holes located 25 mm inside the trachea according to ISO 169005:2016 (ISO 2016A).

Waveforms

Original Waveforms: Tidal volume, V_T (L), and frequency (breathing cycles/min) for the eight ISO sinusoidal breathing rates (Table I) were used to create waveform files (ISO 2016A). Frequencies, checked with a stopwatch, were within 0.5% of specified values. Tidal volumes were measured with a Vitalometer™ water spirometer calibrated with a 1.0 L syringe (Hans- Rudolph, Inc., Shawnee, KS). Tidal volumes were adjusted to within 0.5% of specified values by adjusting the tidal volume input used to create the waveform file as described above.

Revised Waveforms: After the addition of the laser position sensor, measured tidal volume was used to determine adjustments needed for original waveforms as described in Results and Discussion below. Also, for original waveforms (35 and 65 L/min) following errors (when the motor controller cannot track position, stopping the motor) often occurred during transitions between waveforms. This was eliminated when these fractional waveform frequency values, 23.3 and 32.5 cycles (breaths)/min, respectively, were rounded to whole numbers. The tidal volume adjusted proportionally to obtain the specified minute volume, in addition to tidal volume corrections. Minute volumes for revised waveforms were measured with a dry gas meter (DTM 325, American Meter Co.) connected via a Hans-Rudolph series 2700 T-Shape™ Large 2-Way NRB valve. Minute volumes for revised waveforms were within specified tolerance (Table I).

Verification Orifices

ISO WOB method performance is verified both before and after RPD testing: Pressure-volume data is recorded for the ISO waveforms with a verification orifice into the adapter inserted into the trachea as shown in Figure 1A. Orifice A (inner diameter 9.53 mm) is used with the six lowest minute-volume waveforms and orifice B (inner diameter 12.8 mm) with the four highest minute-volume waveforms. Waveforms 65 and 85 L/min are verified with both orifices to provide overlap in the two sets of orifice verification results. Only total volume-averaged WOB (WOB_T/V_T) and asymmetry from these recordings are used. Calculations are discussed below. Verification orifice results are expected to be within ranges specified in ISO 16900–12:2016 for each waveform/orifice combination (Table I) (ISO 2016B). Asymmetry is dependent on the sampling configuration. The verification holder was designed and experimentally evaluated to yield asymmetry with verification orifices generally below 5% (Table I). Asymmetry is not evaluated for RPD.

Work of Breathing Procedure

Test procedure, data treatment and calculations were based on International Standard ISO 16900–12:2016 (ISO 2016B). RPD pressure and volume data was recorded for all eight ISO waveforms run in order of increasing minute volume with a one-minute duration for each waveform. RPD were not pre-conditioned and recorded at ambient conditions.

Respiratory Protective Devices

Purchased RPD were obtained within NPPTL. Most were unused. Used RPD were confirmed to be in working condition according to manufacturer's instructions and assembled as NIOSH-approved configurations. Exceptions were full facepieces with a standard connector that were fitted with a CBRN Cap-1 canister (NIOSH 2007). Filtering facepiece and elastomeric half mask RPD were sealed to the headform with duct tape. Full facepieces indicating face seal leakage were sealed with putty and retested.

Calculations

P-V data for WOB calculations was obtained from recorded data by ensemble averaging (O'Haver 2008). The values for ten consecutive breaths were averaged at each recorded point throughout the period. Volume data was derived from laser position sensor recordings. The relationships used for calculation of volume-averaged total work of breathing (WOB_T/V_T), and asymmetry are summarized in Appendix A. A more thorough discussion is given in Annex B of ISO 16900–12:2016 (ISO 2016B). Calculations were initially performed in Microsoft® Excel 2016 and later in LabVIEW™ (National Instruments, Austin, TX) for incorporation into the data-acquisition function. Results from the later were verified against spreadsheet calculations.

RESULTS AND DISCUSSION

After the breathing machine (above) and piston position measurement changes (Appendix B) were completed, verification orifice results with the original waveforms were obtained. Statistics for preliminary results (n=3) [average, standard deviation and bias] are given in Table II for each waveform/orifice combination.

Average WOB_T/V_T generally agreed with ISO target values (Table I): Only standard deviation for 85/B slightly exceeded one-half the specified range. [This criterion (std. dev. range $(+/-)/2$) was used for excessive variation in that, assuming only random variation, 95% of results are expected to be within the interval: sample average \pm (2x sample std. dev.). Further, assuming specified range (\pm) values are based on the same criteria, standard deviation for samples from a compliant process should not exceed range $(\pm)/2$.] Bias (the relative difference between average and ISO target value as percentage) was within $\pm 5\%$ for all combinations. The overall average absolute bias was 1.7%.

Average asymmetry for combinations 10/A and 20/A did exceed the ISO Specification (Table I). This was likely due to the low signal-to-noise for pressure measurements. The preliminary results indicated the method was likely meeting ISO verification requirements.

Validation, Evaluation and Adjustments

For validation, the original waveforms were then used over a one-month period for about 100 sets of pressure-volume recordings for RPD using the medium 3D-printed ABS ISO RPD head form and a single ISO trachea assembly. The thirty-eight sets of verification orifice recordings also acquired provided a larger sample to reduce uncertainty in the analysis. Statistics for verification orifice WOB_T/V_T and asymmetry (Table III) were derived as above. WOB_T/V_T standard deviation generally increased compared to preliminary results. Only that for combination 35/A (highlighted Table III) was slightly above the excessive variation criterion, range $(+/-)/2$. WOB_T/V_T biases were also greater than preliminary results. Overall average absolute bias was 2.7%, largely due to combinations, 65/A (6.57); 65/B (6.26); 50/A (-3.49); 85/A (2.85); and 35/A (-2.20). In the distribution of WOB_T/V_T results in the specified ISO target \pm ISO range (Table III), the percentage out of range correlated with WOB_T/V_T bias and the large biases (above) reduced percentage within range below the intended 95% (highlighted Table III). Overall 83% of results were within range. Asymmetry for verification orifice results from original waveforms averaged 5.6%, compared to 3.5% for the preliminary results. Combinations with high average asymmetry (excluding 10/A and 20/A) also had large WOB_T/V_T bias. Tidal volume bias (Table III) correlated moderately ($R^2=0.51$) with WOB_T/V_T bias, indicating tidal volumes for revised waveforms should be corrected for tidal volume bias found in the original waveforms.

The revised waveforms were then used in the same way as the original waveforms, in obtaining 225 sets of RPD recordings. Statistics for verification orifice WOB_T/V_T and asymmetry results from fifty-five sets of verification orifice recordings (Table IV) were derived. WOB_T/V_T standard deviations were slightly larger with pooled standard deviation of 0.0373 compared to 0.0336 for original. WOB_T/V_T standard deviation for combination 65/A and 65/B exceeded range $(+/-)/2$: ($0.0506 > 0.0500$) and ($0.0217 > 0.0150$), respectively. Average absolute WOB_T/V_T bias was 1.7, considerably less than original waveforms. Over 97% of WOB_T/V_T results were within range.

Asymmetry for revised waveforms averaged 5.3% due largely to results for combinations 10/A and 85/A. Unlike the original waveform results, the later also had low WOB_T/V_T bias. Overall, asymmetry met specification for 76% of individual results. Excluding 10/A, 20/A, 85/A results, compliance for the remainder was 93%.

To evaluate long-term stability, twenty-four sets of verification WOB_T/V_T and tidal volume results from over a three-month period were statistically analyzed for the effect of test date. No significant differences were found for tidal volume and verification orifice WOB_T/V_T for test date ($p < .05$).

Repeatability of WOB_T/V_T for RPD

To evaluate repeatability of WOB_T/V_T measurements, three RPD chosen from each design class: filtering facepiece, elastomeric half-mask air-purifying, full-facepiece air-purifying, powered air-purifying (hood and full-facepiece), self-contained supplied-air pressure-demand were used. Each was mounted and sealed on the ISO 3 medium ABS headform, WOB_T/V_T was determined at all eight minute ventilation rates for three

repetitions at different times. A repeated measures ANOVA was used to determine if an identifiable difference in mean was observed between the repeated measures. For all minute ventilation rates, no difference in means was identified in the three repetitions for any RPD class ($p < 0.05$).

RPD sealing to reduce face seal leakage is already generally practiced and recommended in the ISO WOB method. To estimate the effect of face seal leakage on WOB_T/V_T , eleven filtering facepiece and three elastomeric half mask respirators were recorded with and then without sealing RPD to the headform. Average WOB_T/V_T for sealed and unsealed RPD was plotted versus minute volume (Figure 3). The percentage decrease in WOB_T/V_T for unsealed versus sealed is shown on the graph. For example, the average WOB_T/V_T measured for unsealed respirator at a minute volume of 85 L/min is 22% less than that of sealed. The overall average decrease was 31%. For each minute ventilation, a paired t-test showed the sealed and unsealed means were significantly different ($p < 0.05$). These results reaffirm that sealing RPD to the head form avoids significant error due to face seal leakage.

Inter-laboratory variability

Preliminary NIOSH NPPTL results in Table I are included in Figure 4 where verification orifice WOB_T/V_T results obtained by five different groups, in Europe and the U.S., using the same trachea assembly are compared with ISO target values. Differences in the mean for each group and ISO target values were examined using student's t-test for each pair and Tukey-Kramer for all pairs at 95% confidence interval. No differences were found significant.

Further Work and Limitations

Although the analysis based on evaluation and adjustment showed that the WOB method described here complies with ISO requirements, refinements will be made to reduce variability. Such reductions would reduce the likelihood of false negatives in RPD conformance testing and benefit leak detection. Further study of the effect of leakage on WOB results will assess the ability to estimate leakage from pressure data. The comparison of preliminary results with other laboratories indicated WOB measurements using ISO-compliant methods will likely agree. Additional inter-laboratory comparisons of both verification orifice and RPD results between laboratories would provide more evidence of that agreement. The repeatability of preconditioned RPD was not evaluated. ISO standards for WOB for RPD specifying pre-conditioning have not been published. Proposed pre-conditioning should be evaluated for the potential to influence WOB.

In keeping with NIOSH NPPTL interests that gave rise to this effort, both a survey of WOB results obtained for current RPD will be reported and comparisons of the ISO WOB method to currently used methods when completed will be reported.

CONCLUSIONS

The objectives of this study were to 1) assemble a WOB method meeting ISO SC15 standards, 2) validate operation and compliance, and 3) assess repeatability for WOB measurements for RPD. These respective conclusions were made: After the revisions

described, the method assembled met ISO standards 16900–5:2016 and ISO 16900–12:2016. Tidal volume can be adjusted to reduce bias in WOB_T/V_T . The method provides consistent compliance during use over time. Absolute bias averaged 1.7% and average coefficient of variation (CV) 2.3%. With sealing to minimize face seal leakage, the ISO-compliant NIOSH NPPTL method described here provides consistent WOB results for RPD that are expected to be comparable to WOB results from others.

Acknowledgements

For contributions indicated below the authors thank the following:

1. Their collaboration (including permission to include round-robin results), feedback, and advice; members of the ISO head form task group: Andrew Viner (Chair), Dan Warkander, David Cowgill, Wolfgang Drews, Andrew Capon, Colleen Miller, Ian Maxwell, Stan Ellis, Troy Baker, Ewa Messaoudi, Graham Bostock, Ziqing Zhuang;
2. ISO RPD headform CAD files and their translation: Wolfgang Drews, Zhipeng Lei, George Niezgoda;
3. 3-D printing; Joe DuCarme, Lee Portnoff;
4. Input and support of the project: Jay Parker, Terry Thornton, Aaron Reeder, Jeffrey Palcic; and
5. Assistance with original waveform generation: Rosalyn King.

Appendix A

Abbreviations and relationships for work of breathing and other P-V parameters

Work of breathing (WOB):

$$WOB = \int P \Delta V$$

V is breathing machine volume.

ΔV the difference in consecutive values: $\Delta V = V_i - V_{i-1}$

Volume-averaged total work of breathing (WOB_T/V_T):

$$WOB_T/V_T = \frac{WOB_T}{V_T}$$

Tidal volume (V_T): $V_T = |V_{max} - V_{min}|$

Total work of breathing (WOB_T): $WOB_T = WOB_{in} + WOB_{ex}$

Inspiratory work of breathing (WOB_{in}): $WOB_{in} = \int_{V_{min}}^{V_{max}} (P - EV) \Delta V$

Expiratory work of breathing (WOB_{ex}): $WOB_{ex} = \int_{V_{max}}^{V_{min}} (P + EV) \Delta V$

$$\text{Elastance (E): } E = \left(\frac{P_{V_{min}} - P_{V_{max}}}{V_T} \right)$$

Pressure at minimum volume ($P_{V_{min}}$)

Pressure at maximum volume ($P_{V_{max}}$)

Asymmetry:

$$\text{Asymmetry} = 100 * \left| 1 - \frac{P_{max}}{P_{min}} \right|$$

Pressures:

Maximum expiratory pressure (P_{max})

Minimum inspiratory pressure (P_{min})

Further description is found in ISO 16900–12:2016 (ISO 2016B).

Appendix B

Leak tightness

Applying the pressure-decay leak check, ISO 16900–5:2016 Section 4.3.2.5, (ISO 2016A), one breathing machine that met the requirement was identified from several with no leak specifications. As the selected breathing machine was used, the piston seal, and later the shaft seal, began leaking. The original piston seal was replaced with a BUNA O-ring. Shaft seal leakage was obviated by inverting the breathing machine and using the lower cylinder chamber (Figure 1A).

After further use, below-range verification orifice results indicated leakage that was confirmed by the pressure-decay leak check. When the piston was removed, the replacement O-rings were puckered in the channel, and leak paths indicated by the pattern of lubricant on the cylinder wall. Compared to unused O-rings, the used O-rings outer diameter was greater. The petroleum-based grease used for lubricating the O-rings was swelling the BUNA rubber. It was replaced with a silicone-based grease. The breathing machine cylinder is steel. Prolonged contact with water (e.g. leak check solutions) unknowingly introduced into the cylinder resulted in rust and pitting.

Piston position

Initially, piston position (displacement) information for volume was to be obtained from the linear potentiometer. This approach was set aside due to high noise levels in the potentiometer output. In the interim, waveform volume from the waveform file was used. The pressure-volume curve (top graph in Figure 2) gave WOB values consistently lower than expected. When plotted versus time (Figure 2 bottom graph) a difference between

the waveform volume and piston position-derived volume is evident; the waveform file volume runs ahead of the measured position. This difference also varied slightly between waveforms. After installing the non-contact laser-triangulation position sensor, WOB values from the resulting pressure-volume plot (Figure 2 middle graph) were in good agreement with expected values. Accurate volume data requires direct piston-position measurement (paragraph 7.2 of ISO 16900–12). The noisy potentiometer, along with the original motor assembly, was later replaced. These potentiometer-derived volume results (Figure 2 bottom graph) were in phase with the laser position sensor-derived results.

Linear potentiometer comparison to laser position sensor

To evaluate the utility of linear potentiometer output, ensemble-averaged volumes (in liters) were calculated from both linear potentiometer and laser position sensor data from eleven recordings of ISO waveform/verification orifice combinations. The two sets of volume results for each recording were compared by linear regression analysis. Average results (and standard deviation) were:

slope, 1.003 (0.056); Intercept, 0.024 (0.019);

slope standard error, 0.0022 (0.0004); intercept standard error, 0.0023 (0.0005);

R^2 , 0.999 (0.0012);

standard error for y estimate, 0.0195 (0.0013); and

data pairs, 244 (129).

The high correlation between volumes derived from each source show the functional potentiometer provided equivalent volume results.

Verification orifice cautions

Control software at times (e.g. on initialization) abruptly changed piston position. These rapid changes during expiration occasionally expelled the orifice holder and the orifices with a small trajectory. In addition to protecting items below the trachea, software modifications were made to eliminate rapid position changes. The original 3D-printed verification orifice holders with integral seals when replaced with steel holders with O-ring seals providing tighter fit, prevented ejection. As the lower edges of the steel orifice holders are sharp and have the potential to be ejected, personnel should not be in front of the machine when the breathing machine is running.

REFERENCES

- CEN (2003). EN 14143:2003 E Respiratory equipment – Self-contained re-breathing diving apparatus, European committee for standardization (CEN).
- Bentley AR , Oliver OG, Love RG, Muir DC and Sweetland KF (1973) “Acceptable Levels for Breathing Resistance of Respiratory Apparatus.” *Archives of Environmental Health: An International Journal* 27(4): 273–280.

- Caretti DM and Whitely JA (2006). "Exercise performance during inspiratory resistance breathing under exhaustive constant load work." *Ergonomics* 41(4): 501–511.
- ISO (2012). ISO TS 16976–4-2012 Respiratory protective devices - Human factors - Part 4: Work of breathing and breathing resistance: Physiologically based limits, International Organization for Standardization (ISO).
- ISO (2015A). ISO 16900–13 Respiratory protective devices - Methods of test and test equipment — Part 13: RPD using regenerated breathable gas and special application mining escape RPD: Consolidated test for gas concentration, temperature, humidity, work of breathing, breathing resistance, elastance and duration, International Organization for Standardization (ISO).
- ISO (2015B). ISO TS 16976–2-2015 Respiratory protective devices - Human factors - Part 2: Anthropometrics, International Organization for Standardization (ISO).
- ISO (2016A). ISO 16900–5 Respiratory protective devices - Methods of test and test equipment – Part 5: Test equipment – Breathing machine, metabolic simulator, RPD headforms/torso, tools and transfer standards, International Organization for Standardization (ISO).
- ISO (2016B). ISO 16900–12 Respiratory protective devices – Methods of test and test equipment — Part 12: Determination of volume-averaged work of breathing and peak respiratory pressures, International Organization for Standardization (ISO).
- NIOSH (2007). Statement of Standard for Chemical, Biological, Radiological, and Nuclear (CBRN) Full Facepiece Air Purifying Respirator (APR). National Institute for Occupational Safety and Health (NIOSH). From <https://www.cdc.gov/niosh/npptl/standardsdev/cbrn/APR/standard/pdfs/aprstdA.pdf>.
- O’Haver T. (2008). "Intro. to Signal Processing:Signal and Noise [Ensemble averaging]." A Pragmatic Introduction to Signal Processing from <http://terpconnect.umd.edu/~toh/spectrum/SignalsAndNoise.html#EnsembleAveraging>.
- Positek. (2017). "LIPS P101 stand-alone linear position sensor." from <http://www.positek.com/products/p100-cylinder-linear-position-sensor?mfp=2f-measurementtype%5B4%5D>.
- Shykoff BE and Warkander DE (2011). "Physiologically acceptable resistance of an air purifying respirator." *Ergonomics* 54(12): 1186–1196. [PubMed: 22103726]
- Silverman LLG; Drinker K; Carpenter T (1943). Fundamental factors in the design of protective respiratory equipment, Harvard School of Public Health.
- Warkander DE (2015). Breathing Machines for Work of Breathing, US Naval Experimental Diving Unit.
- Warwick_Technology. (2013). "Warwick Technology Digital Breathing Machine." Retrieved 6/27/2016, from <http://breathingmachine.co.uk/>.

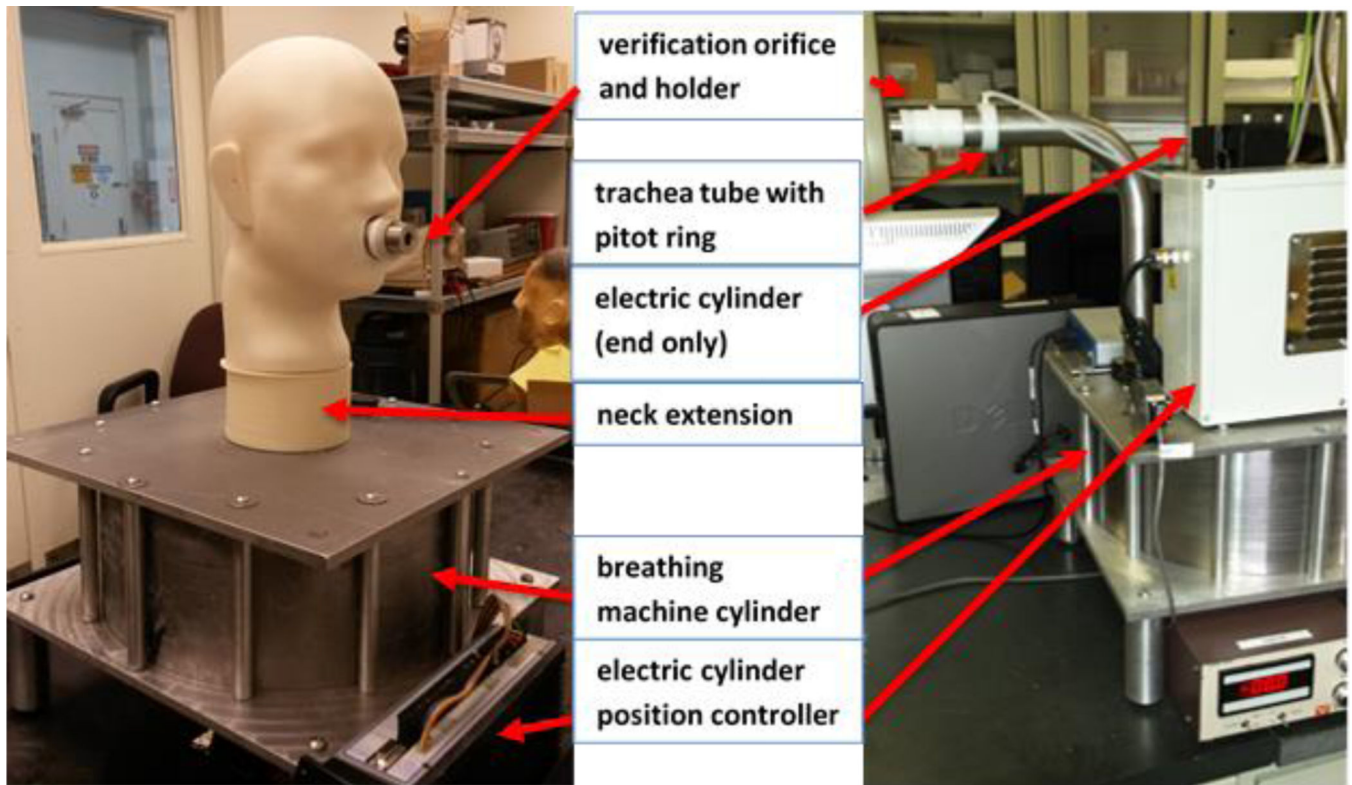


Figure 1.

A (left) - Medium ISO headform 3 supported on spacer with trachea tube assembly (not visible) connected to inverted breathing machine; B (right) - ISO trachea tube assembly with verification orifice attached to original breathing machine.

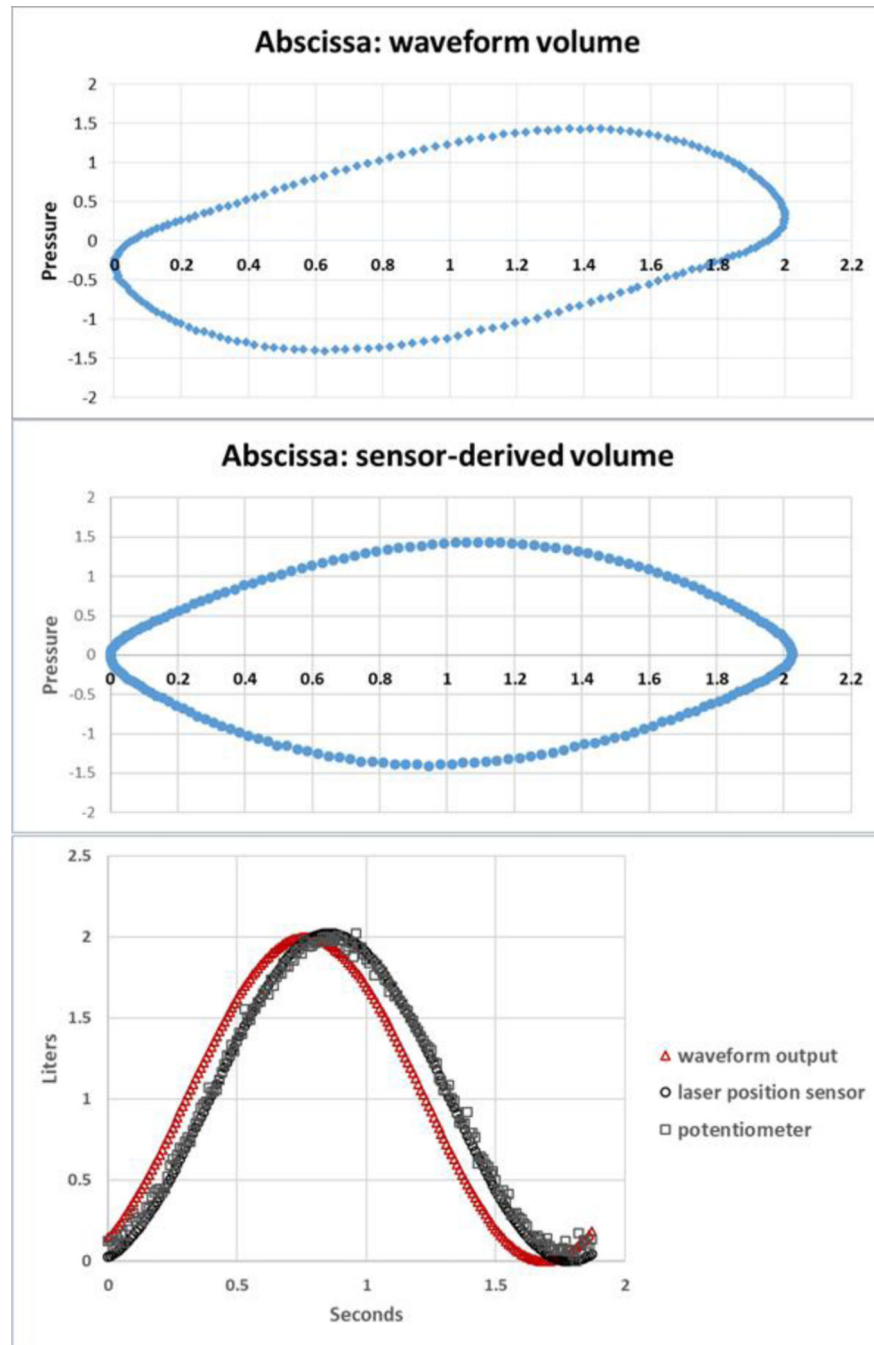


Figure 2. Top: Pressure-volume results using waveform file-derived volume; Middle: Pressure-volume results using laser position sensor-derived volume; and Bottom: Comparison of volume from waveform, laser position sensor and potentiometer versus time, showing phase difference (Appendix B).

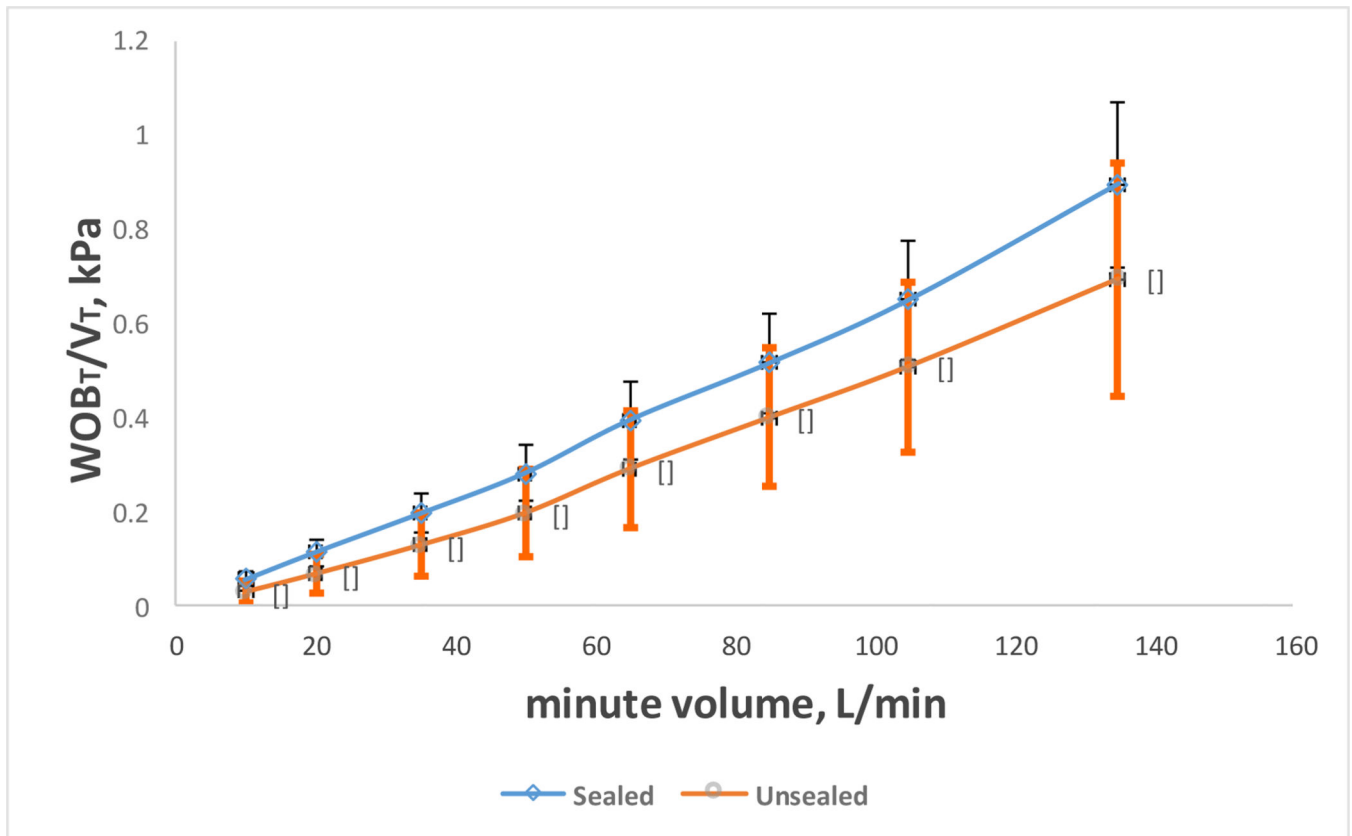


Figure 3. Average WOB_T/V_T for half-mask respirators (n=11) sealed and unsealed versus waveform minute volume. Numbers on graph are the percentage decrease in average WOB_T/V_T for unsealed relative to sealed. Error bars represent standard deviation.

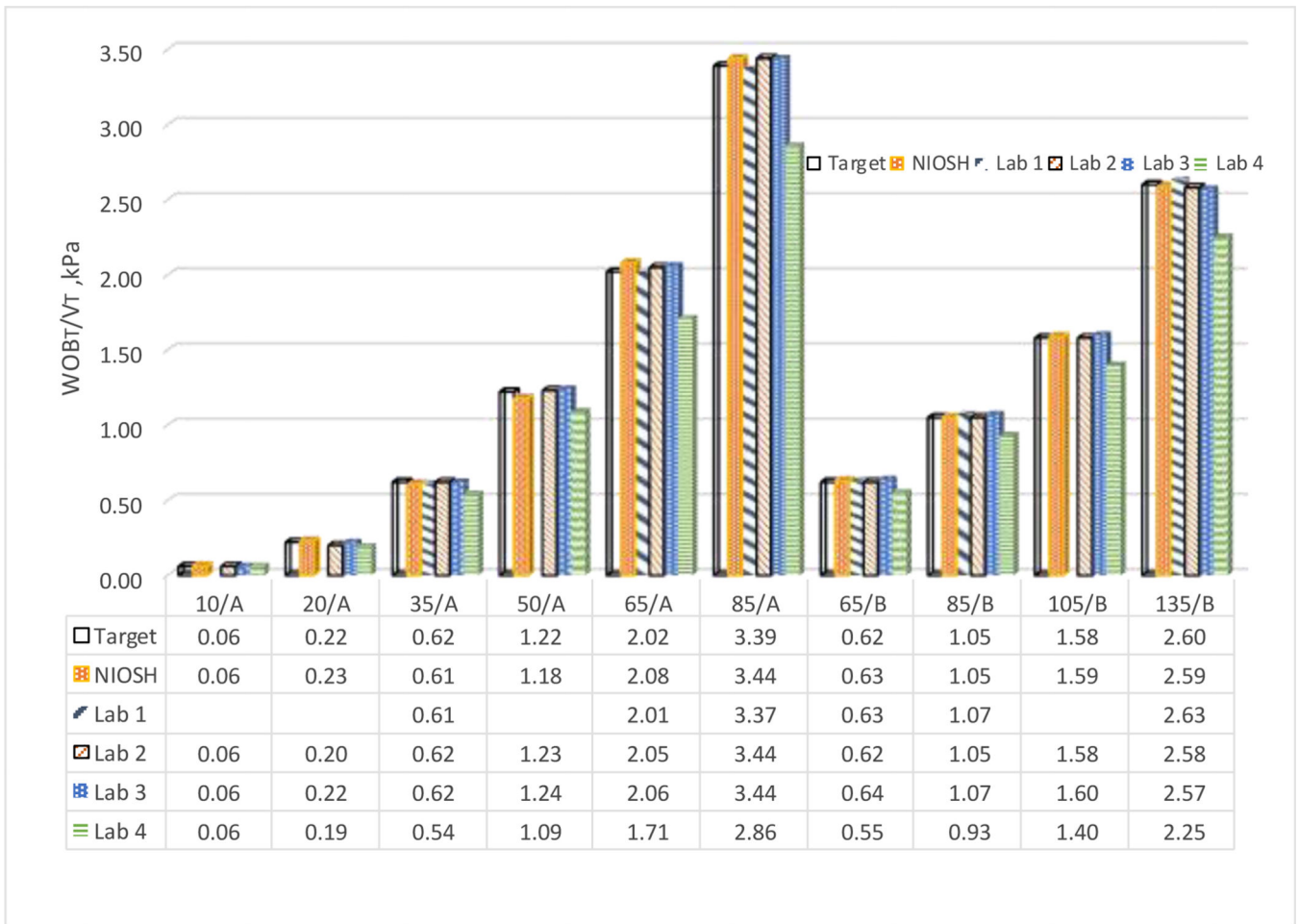


Figure 4. Verification orifice WOB_T/V_T results from five laboratories and ISO target values.

Table I.

Specifications for Waveforms, Verification Orifice WOB_T/V_T and Asymmetry by Waveform/orifice Combination

Waveform /Orifice combination (minute volume/orifice)	Waveforms			Verification orifice		
	(ISO 16900-5:2016)			(ISO 16900-12:2016)		
	Minute volume tolerance (%)	Tidal volume (L)	Frequency (min^{-1})	WOB_T/V_T (kPa)		Asymmetry %
target				range (\pm)		
10/A	3	1.0	10	0.06	0.01	8
20/A	2	1.0	20	0.22	0.02	5
35/A	2	1.5	23.3	0.62	0.03	5
50/A	2	2.0	25	1.22	0.06	5
65/A	2	2.0	32.5	2.02	0.10	5
85/A	2	2.5	34	3.39	0.17	5
65/B	2	2.0	32.5	0.62	0.03	5
85/B	2	2.5	34	1.05	0.05	5
105/B	1	2.5	42	1.58	0.08	5
135/B	1	3.0	45	2.60	0.13	8

Table II.

Verification Orifice WOB_T/V_T and Asymmetry: Preliminary Results for Original Waveforms Values by Waveform / Orifice Combination

Waveform / Orifice combination designation	Verification orifice results statistics					
	Preliminary results (n=3)					
	WOB _T /V _T (kPa)			Asymmetry		
	avg.	std. dev.*	%bias**	avg.***	std. dev.	
10/A	0.063	0.0034	5.0	14.6	12.2	
20/A	0.23	0.0045	4.6	5.9	5.5	
35/A	0.61	0.0044	-1.6	2.0	1.1	
50/A	1.18	0.0109	-3.3	1.2	0.7	
65/A	2.08	0.0182	3.0	2.3	1.0	
85/A	3.44	0.0341	1.5	3.6	1.3	
65/B	0.63	0.0076	1.6	2.0	2.0	
85/B	1.05	0.0276	0.0	1.2	1.0	
105/B	1.59	0.0196	0.6	0.7	0.8	
135/B	2.59	0.0352	-0.4	1.5	0.7	

* Standard deviations exceeding half the specified range (std.dev. > range /2) are highlighted.

** %bias = 100*(avg.-target)/target.

*** Average asymmetry greater than ISO specification (Table I) are highlighted.

Table III.

Statistics for Verification Orifice Results and Measured Tidal Volumes throughout Testing Using Original Waveforms

Waveform / orifice combination	Verification orifice results statistics					WOB _T /V _T distribution in specified range [^]			Tidal volume statistics		
	WOB _T /V _T (kPa)			Asymmetry (%)		%			liters		
	avg.	std. dev.*	% bias**	avg ****	std. dev.	below	within***	above	avg.	std. dev.	%bias**
10/A	0.062	0.0026	2.52	15.8	12.3	0	100	0	0.99	0.0171	-1.33
20/A	0.22	0.0052	0.36	5.1	4.2	0	100	0	1.00	0.0196	0.05
35/A	0.61	0.0151	-2.20	6.7	2.1	8	92	0	1.50	0.0225	-0.16
50/A	1.18	0.0224	-3.49	4.3	1.5	16	84	0	1.96	0.0929	-2.18
65/A	2.15	0.0416	6.57	6.7	1.4	0	26	74	2.08	0.0273	3.85
85/A	3.49	0.0668	2.85	6.8	2.6	0	89	11	2.51	0.0851	0.60
65/B	0.66	0.0129	6.26	1.5	1.1	0	44	56	2.03	0.0083	3.85
85/B	1.07	0.0210	1.74	4.2	1.8	0	95	5	2.53 ^{^^}	0.0320 ^{^^}	1.21 ^{^^}
105/B	1.58	0.0332	-0.21	3.9	1.8	0	100	0	2.50	0.0290	-0.02
135/B	2.58	0.0509	-0.75	3.7	1.4	1	99	0	2.99	0.0324	-0.34

* Standard deviations exceeding half the specified range (std. dev. > range/2) (Table I) are highlighted.

** %bias = 100*(avg.-target)/target.

*** Percentages less than 95 are highlighted.

**** Average asymmetry greater than ISO specification (Table I) are highlighted.

[^] Range = ISO target +/- ISO range (±). (Table I).

^{^^} Statistics for nine results.

Table IV.

Statistics for Verification Orifice Results throughout Testing Using Revised Waveforms

Waveform / orifice combination	Verification orifice results statistics					WOB _T /V _T distribution in specified range [^]		
	WOB _T /V _T (kPa)			Asymmetry (%)		%		
	avg.	std. dev.*	% bias**	avg.***	std. dev.	below	within***	above
10/A	0.062	0.0035	3.78	21.1	17.5	0	100	0
20/A	0.23	0.0047	3.68	5.0	6.4	0	100	0
35/A	0.61	0.0131	-2.00	3.5	2.2	5	95	0
50/A	1.20	0.0251	-1.94	3.3	1.8	5	95	0
65/A	2.01	0.0506	-0.32	4.3	1.1	2	96	2
85/A	3.40	0.0744	0.39	7.1	1.2	2	96	2
65/B	0.61	0.0217	-1.60	2.4	1.6	4	93	3
85/B	1.04	0.0242	-0.93	1.9	1.4	2	98	0
105/B	1.59	0.0303	0.83	2.1	1.2	0	100	0
135/B	2.63	0.0554	1.26	2.3	1.1	0	96	4

* Standard deviations exceeding half the specified range (std. dev. > range/2) (Table I) are highlighted.

** %bias = 100*(avg.-target)/target.

*** Percentages less than 95 are highlighted.

**** Average asymmetry greater than ISO specification (Table I) are highlighted.

[^] Range = ISO target +/- ISO range (±) (Table I).